

Automatic Classification of Roof Shapes for Multicopter Emergency Landing Site Selection (Extended Abstract)

Jeremy D. Castagno* and Ella M. Atkins†
University of Michigan, Ann Arbor, MI, 48109

I. Introduction

GEOGRAPHIC information system (GIS) data is openly available for a variety of applications. Data on terrain height has historically been available; high-accuracy labelled data is now also available, e.g., indicating building footprints and heights. Unmanned Aircraft Systems (UAS) offer low-cost airborne data collection and small payload transport capabilities to support a variety of missions including but not limited to urban mapping [1]. Routine small UAS operation over urban regions requires mitigation of risk posed to overflown people and property. Small UAS are envisioned to operate at low altitudes, below the airspace occupied by manned aircraft. In a congested environment, the low-flying UAS will operate near buildings thus will have little time or space to execute a "safe ditching" (emergency landing) given an unrecoverable anomaly or failure [2]. Concise and accurate information of nearby landing sites, including building rooftops, is needed in these situations. Databases such as OpenStreetMap (OSM) (<https://www.openstreetmap.org/>) and Mapbox (<https://www.mapbox.com/>) provide open data on infrastructure as well as terrain. Roof geometry is offered as a possible field in OSM that could provide information for a small UAS; however, roof geometry and architecture (type) information is often missing or incomplete in these existing databases. This paper provides missing roof type classification information from publicly-available GIS data.

This paper fuses satellite imagery and LIDAR data through multiple stages of machine learning classifiers to accurately characterize building rooftops. With these results, roof geometries worldwide can be stored in an easily-accessible format for UAV and other applications. Supervised training datasets are automatically generated by combining OSM, satellite, and LIDAR data. The resulting annotated dataset provides individual satellite image and LIDAR image representations for each building roof. Roof shapes are automatically labelled through a novel combination of convolutional neural networks (CNNs) using these roof images from satellite and LIDAR data sources. Transfer learning is employed in which pre-trained CNN model architectures and hyper-parameters are fine-tuned and tested. The best performing CNN for both satellite and LIDAR data inputs is used to extract a reduced feature set which is then fed into support vector machine (SVM) and random forest classifiers to extract a single roof geometry decision. Validation and test set accuracies are evaluated over a suite of different classifier options. Imagery and roof classification data from Witten, Germany is used in this work based on prior availability of human-input (crowd-sourced) roof geometry classification data for buildings throughout the region.

II. Background

Satellite color images and 3D point cloud data from airborne Light Detection and Ranging (LIDAR) sensors provide complementary roof information sources. High resolution satellite images offer rich information content and are generally available worldwide. However, extracting 3D building information from 2D images is difficult due to occlusion, poor contrast, shadows, and skewed image perspectives [3]. Raw LIDAR sensors provide depth and intensity measurements generating a 3D point cloud capturing the features of roof shapes, yet LIDAR does not offer other world feature information from ambient lighting intensity and color. LIDAR point cloud data is often processed and converted to digital surface models (DSM) representing the top surface layer of any terrain.

The UAV localization and emergency landing application targeted by this paper only requires a simple classification of a building roof shape. In fact, complex model representations are undesirable given that a UAV emergency landing plan to a flat rooftop, for example, would be computed by a low-power lightweight embedded processor. Classical machine learning algorithms such as support vector machines (SVM), logistic regression, and decision trees are often used in these classification scenarios but invariably face computational complexity challenges caused by the high

*J. D. Castagno is with the Department of Aerospace Engineering, University of Michigan, Ann Arbor, MI, 48109 USA e-mail: jdcasta@umich.edu.

†E. M. Atkins is with the Department of Aerospace Engineering, University of Michigan, Ann Arbor, MI, 48109 USA e-mail: ematkins@umich.edu.

dimensionality found in these GIS data sources. Deep learning, through the use of techniques such as convolutional neural networks (CNN), have demonstrated the ability to accurately and robustly classify high dimensional data sources such as camera images [4]. The GIS community has begun to apply CNNs to roof identification. Perhaps most closely related to this paper, Alidoost and Arefi (2016) trained CNNs using satellite (RGB) and digital surface map (DSM) images to label basic roof shapes [5]. However the final predicted roof shape was simply taken as the highest probability result between the two models. Patrovi et. al [6] fine-tuned a CNN using patched satellite images of building roof-tops. Using the fine-tuned CNN, the authors extracted high-level features of images as inputs to a second-stage SVM classifier. This paper adopts an analogous two-stage processing approach to roof classification with the addition of LIDAR and satellite feature fusion. Specifically, this fusion allows the creation of a nonlinear decision function that exploits the strengths of each modality. Note that the full paper will contain additional background on CNNs in the context of RGB and LIDAR feature detection and classification problems.

III. GIS Roof Data Extraction and Processing

To classify roof geometries, a large annotated data set must be processed and randomly split into distinct training, validation, and testing subsets. This paper relies on a fusion of OSM, satellite imagery, and airborne LIDAR data sources to generate this data set. Each building roof is classified based on corresponding satellite (RGB) and LIDAR images of the roof top.

A. Classified Image Set Generation

Generation of an annotated roof data set requires three data sources for each building: satellite RGB imagery, airborne LIDAR data, and building outlines with corresponding roof labels (from manual classification). All three of these data sources must be properly geo-referenced so they can be fused together. Care must be taken to select a geographic area where data sources for all of these items are present, as well as a sufficiently dense number of pre-labeled buildings. OpenStreetMap (OSM) provides the necessary building outlines in almost all geographic regions, however the associated roof shape label is often not complete. Some geographic regions (e.g. Germany) are more likely to have a denser collection of labeled roof shapes through a higher volunteer involvement. Once the appropriate data sources have been found, the methods described below can be employed to extract satellite and LIDAR images for each building.

Satellite, LIDAR, and OSM data sources have their own spatial reference systems (SRS). The SRS defines a map projection and determines the transformations needed to convert to a different SRS. These reference systems are uniquely identified through a spatial reference system identifier (SRID) which designates an authority and an identifier. For example, the European Petroleum Survey Group (EPSG) can be used to specify SRID's. OSM chooses to store building outlines as polygons, with each vertex stored in WGS84 (EPSG:4326). Satellite images from common map vendors (ArcGIS, Bing, Google) often use WGS84 / Pseudo-Mercator (EPSG:3857). LIDAR data is usually stored in a region-specific SRS; data for Witten, Germany uses EPSG:5555. To convert a point stored in one SRS to another, a program specialized in these transformations, such as `proj.4`, must be used. OSM building polygons are transformed to their LIDAR and satellite counterpart coordinate systems so that the building outlines are consistent.

1. LIDAR Image Construction

A bounding box (BBOX) is constructed from the polygon building outline provided by OSM. This BBOX is used first to quickly filter out points in the LIDAR data set not related to the building of interest. The resulting subset of points is filtered again using the polygon roof outline, resulting in only points encapsulated in the building outline. At this time, the 3D LIDAR point cloud is noisy and may contain undesirable points, especially near the edges of the outline (i.e. wall hits). To remove these outliers, the points' z -coordinates are used to analyze their distribution. A robust metric for outlier removal is to use the median absolute deviation (MAD) and construct a modified z -score that measures how deviant each point is from the MAD [7]. This method only applies to unimodal distributions; however not all buildings height are distributed as such. For example, there exist complex flat buildings that contain multiple height levels resulting in a multimodal distribution. To distinguish these buildings the dip test statistic is employed which measures multi-modality in a sample distribution [8]. Any building with a dip statistic less than .04 or with a p -value greater than .2 is considered unimodal, and outlier removal is performed.

Once LIDAR point extraction is complete, the points are projected onto a plane, creating a 2D grid that takes the value of each point's height information. The 2D grid world dimensions are the same as the bounding box of the buildings, with the discrete grid size being the desired square image resolution. Grid points use interpolation of nearest

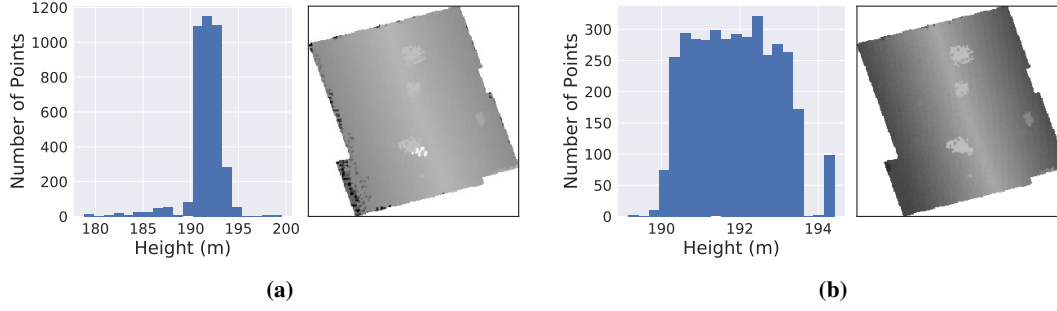


Fig. 1 LIDAR data of a gabled roof. Histogram of height distribution and generated image (a) before filtering and (b) after filtering, using median absolute deviation.

neighbor if no point is available. Afterward this grid is converted into a grayscale image, where each value is scaled from 0-255 with higher values whiter and lower areas darker. Examples of this filtering are shown in Figure 1. The CNNs used in this paper require the grayscale LIDAR data be converted to a three-channel RGB image by duplicating the single channel across all three color channels. This final image is referred to as the LIDAR image.

2. Satellite Image Construction

Satellite RGB (red-green-blue) images must have a minimum ground resolution of 1m, however sub-meter resolution is recommended. It is preferable that the imagery be ortho-rectified to remove image tilt and relief effects. Ideally the OSM building polygon can be used to completely *stamp* out a roof shape image. However, if the aforementioned issues are present in the image, it is unlikely that the OSM polygon will exactly match the building outline in the image. This was the case when using ArcGIS world imagery for the city of Witten, Germany. To work around these issues, an enlarged crop can be made around the building. The enlarged crop is produced by orthogonally expanding each edge of the building polygon by a configurable constant, and then using the bounding box of the new polygon as the identifying stamp. After experimentation, this configurable constant was set to three meters when processing the Witten data set. After the image is produced, the image is resized to the square image resolution required by the CNN.

B. CNN Architectures and Training

The CNN base architectures chosen for experimentation are VGG16 [9], Resnet50 [10], and Inceptionv3 [11]. All three of these architecture structures are distinct; when trained and tested on ImageNet they received "top 5" accuracy scores of 89.8%, 92.8%, and 93.9% respectively. Each CNN makes use of successive convolutional blocks to generate a final feature map (referred to as the base layers) which are subsequently used by downstream fully-connected layers to make a 1000 categorical prediction (referred to as the top layers). The top layers are domain specific and are not needed for the roof classification task. Three new architecture templates are constructed using the pre-trained CNN base layers: a flattening layer, a fully connected layer (FC1), and a softmax prediction layer as shown in Figure 2. Additionally the size of FC1 is also varied over vector lengths of 25, 50, and 100. These models are then subsequently trained individually on the RGB and LIDAR images.

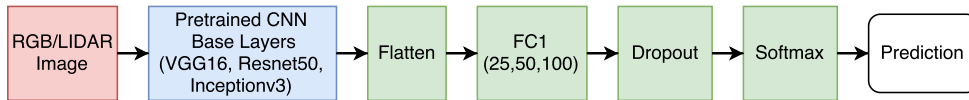


Fig. 2 CNN Architecture Templates

Training will initialize the weights for the base layers with their respective parent architecture. The optimizer chosen for gradient descent is Adadelta [12] for its ability to effectively adjust the learning rate automatically for individual weights; this optimizer is kept consistent for all architectures and training sessions. The option of freezing initial layers is exploited with a variable number of frozen layers chosen. When layer 11 is said to be frozen, this means all previous layers, (1-11), are frozen during training. All base architectures and tested hyper-parameters are shown in Table 1.

After training is complete on all CNN architectures and hyperparameters, the best performing CNN with respect to

Table 1 CNN Architectures and Hyperparameters

Base CNN Model	FC1 Size	Frozen Layers
VGG16	25,50,100	11, 15
Resnet50	25,50,100	50, 80
InceptionV3	25,50,100	18, 87

Table 2 SVM and Random Forest Training Configurations

Classifier	Parameters
SVM	C: 1,10,100 Kernel: linear,rbf,poly,sigmoid
Random Forest	Criterion: gini, entropy Num Estimators: 5,10,50 Max Depth: 5,10,50

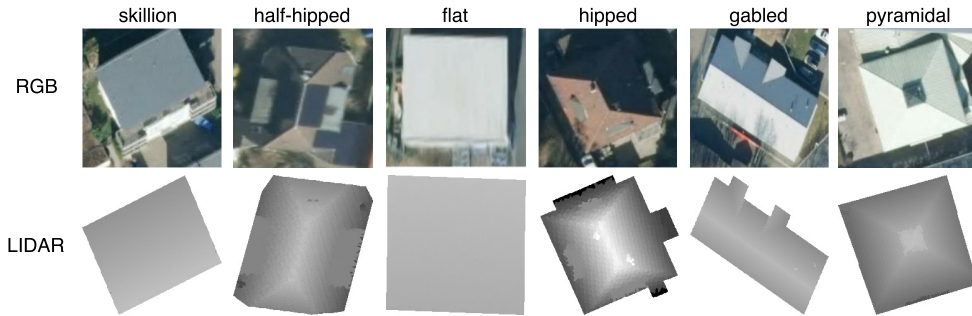
the validation set accuracy for both LIDAR and RGB images is selected for use in feature extraction and subsequent training with SVM and random forest classifiers. In this scenario only the layers including and before FC1 are used to generate a condensed feature map the size of FC1 to represent the image. The augmented training set images are *reduced* to this small feature vector, and are used to train both sets of classifiers over a variety of configurations as shown in Table 2.

IV. Results

A. Case Study and Data Set Generation

The geographic region of interest chosen for analysis was the city Witten in the North Rhine-Westphalia state (NWR) of Germany. The state of NWR has recently (May 2017) made public their full LIDAR data set with a permissible license [13]. In addition the city of Witten has the desirable characteristic of having the most densely-labeled roof shapes in the OSM database, providing a robust pre-labeled data set for this paper’s analysis. Satellite images were garnered through using ArcGIS world imagery base maps with ground resolution of 0.2 meters.

In the city of Witten the most prevalent roof shapes were Flat, Gabled, Hipped, Half-hipped, Skillion, and Pyramidal. All other roof shapes did not provide a sufficient number of samples (minimum 100 samples) to be used for supervised training. A total of 26,719 buildings have the above-mentioned roof shapes, and RGB and LIDAR images were generated for all buildings. Examples of generated images can be found in Figure 3. To ensure an accurate data set would be used for training, validation, and testing, 2500 buildings were randomly selected for review and manually removed if any issues were detected. Out of the 2500 buildings, 1119 were removed for reasons such as: poor LIDAR image quality, trees obscuring the roof, and the building being absent (demolished). The remaining 1381 buildings were randomly split 60/30/10 into training, validation, and test sets, respectively.

**Fig. 3 Example of generated images**

B. CNN Training and Results

Training was performed on the University of Michigan’s Flux system, providing a server with six gigabytes of RAM, two CPU cores, and an NVIDIA Tesla K20X. A graphical overview of results over all evaluated CNN architectures and hyperparameters for LIDAR and RGB inputs can be found in Figure 4a and 4b, respectively. Each dot represents a

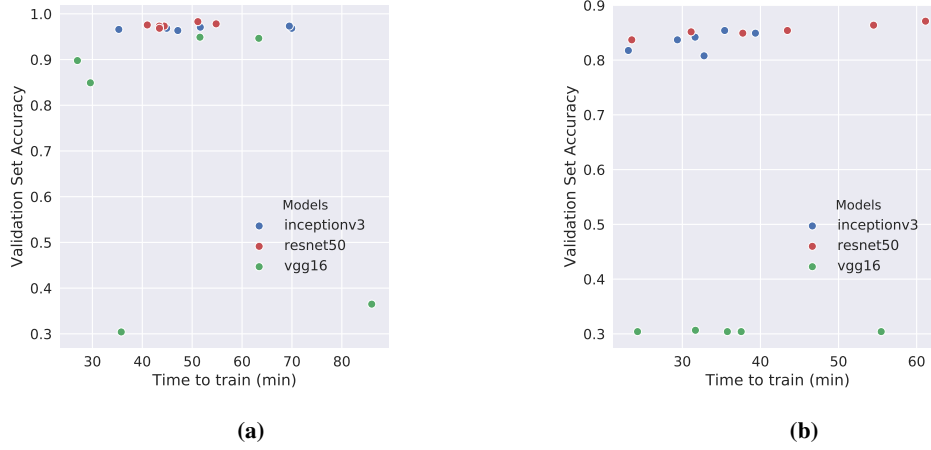


Fig. 4 (a) Validation set accuracy with LIDAR input. (b) Validation set accuracy with RGB image input.

configured training session, with the color denoting the base model architecture used, while the FC1 size and frozen layers parameters are not shown. The vertical axis shows *validation* set accuracy and the horizontal axis is the amount of time taken to train a model.

The most successful base model architectures were Resnet50, Inceptionv3, and finally VGG16 with a relatively poor performance. The top performing model architecture for LIDAR and RGB inputs was actually the same Resnet50 model with a FC1 size of 100 and all 50 initial layers frozen during training. These models gave a validation accuracy of 98.3% and 87.1% for LIDAR and RGB inputs respectively. These results demonstrates good generalizability of the models, and leads us to select them for use in feature extraction as inputs with SVM and decision tree classifiers.

C. Feature Extraction and Classification Training and Testing

The same training set is processed with the fine-tuned Resnet50 model to produce a condensed feature set for each building image, both LIDAR and RGB. After this processing, each building's LIDAR and RGB image is represented by a feature vector of length 100. This new high level feature training set is then fed to SVM and random forest classifiers with varied configurations. Once all classifiers are trained, they are run against the *test* data set with results shown in Figure 5. The fine-tuned Resnet50 model is shown in red for comparison.

These results indicate that the test accuracy is able to improve modestly, around 1.4% in the best case, by combining both the RGB and LIDAR feature sets into one fused dual input. This illustrates the ability of these algorithms to learn a nonlinear decision function that can account for the strengths and weaknesses of LIDAR and RGB data. In essence, fused data results are better than either LIDAR or RGB data alone. Table 3 highlights the top performing models, parameters, and test set accuracies.

V. Discussion and Conclusions

This paper proposed fusing a combination of OpenStreetMap (OSM), satellite, and LIDAR data to generate images of buildings and predict roof shapes (types). Pre-labeled data from OSM was exploited to auto-generate a training dataset. Multiple CNN architectures were trained and tested, with the highest-performing CNN selected for image feature extraction for use with second stage SVM and decision tree classifiers. The combination of RGB and LIDAR image features support previous findings that multi-modality data fusion can improve classification accuracy. In future work, we will contribute automatically-generated roof shape labels to the OSM database. This information can be used to find safe landing sites in autonomous UAV emergency landing scenarios. Additional results and algorithm details will be presented in the full paper.

Acknowledgment

This work was in part supported under NASA Award NNX11AO78A and NSF Award CNS 1329702.

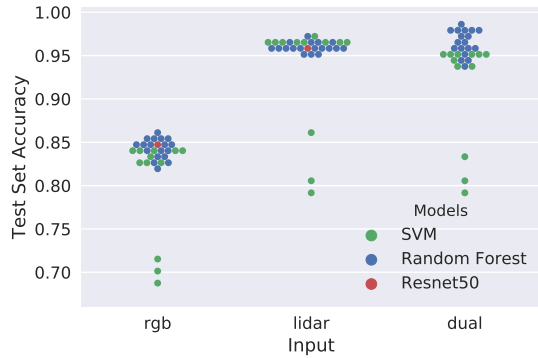


Table 3 Best performing feature classifiers and their associated test set accuracies. RF=Random Forest, C=Criterion, NE=Number of Estimators, MD=Maximum Depth

Input	Accuracy	Model	Parameters
rgb	.861	RF	C: gini, NE: 5, MD: 50
lidar	.972	RF	C: gini, NE: 5, MD: 10
dual	.986	RF	C: gini, NE: 50, MD: 50

Fig. 5 Test data set accuracies for feature extraction and training on SVM and decision tree classifiers.

References

- [1] Thomas, N., Hendrix, C., and Congalton, R. G., "A comparison of urban mapping methods using high-resolution digital imagery," *Photogrammetric Engineering & Remote Sensing*, Vol. 69, No. 9, 2003, pp. 963–972.
- [2] Ochoa, C. A., and Atkins, E. M., "Fail-Safe Navigation for Autonomous Urban Multicopter Flight," *AIAA Information Systems-AIAA Infotech@ Aerospace*, 2017, p. 0222.
- [3] Zhou, G., and Zhou, X., "Seamless fusion of LiDAR and aerial imagery for building extraction," *IEEE Transactions on Geoscience and Remote Sensing*, Vol. 52, No. 11, 2014, pp. 7393–7407.
- [4] Schmidhuber, J., "Deep learning in neural networks: An overview," *Neural networks*, Vol. 61, 2015, pp. 85–117.
- [5] Alidoost, F., and Arefi, H., "KNOWLEDGE BASED 3D BUILDING MODEL RECOGNITION USING CONVOLUTIONAL NEURAL NETWORKS FROM LIDAR AND AERIAL IMAGERIES," *International Archives of the Photogrammetry, Remote Sensing & Spatial Information Sciences*, Vol. 41, 2016.
- [6] Partovi, T., Fraundorfer, F., Azimi, S., Marmanis, D., and Reinartz, P., "Roof Type Selection based on patch-based classification using deep learning for high Resolution Satellite Imagery," *International Archives of the Photogrammetry, Remote Sensing and Spatial Information Sciences-ISPRS Archives*, Vol. 42, No. W1, 2017, pp. 653–657.
- [7] Iglewicz, B., and Hoaglin, D., *How to Detect and Handle Outliers*, ASQC basic references in quality control, ASQC Quality Press, 1993. URL <https://books.google.com/books?id=siInAQAAIAAJ>.
- [8] Hartigan, P., "Algorithm AS 217: Computation of the dip statistic to test for unimodality," *Journal of the Royal Statistical Society. Series C (Applied Statistics)*, Vol. 34, No. 3, 1985, pp. 320–325.
- [9] Simonyan, K., and Zisserman, A., "Very Deep Convolutional Networks for Large-Scale Image Recognition," *CoRR*, Vol. abs/1409.1556, 2014. URL <http://arxiv.org/abs/1409.1556>.
- [10] He, K., Zhang, X., Ren, S., and Sun, J., "Deep Residual Learning for Image Recognition," *arXiv preprint arXiv:1512.03385*, 2015.
- [11] Szegedy, C., Vanhoucke, V., Ioffe, S., Shlens, J., and Wojna, Z., "Rethinking the Inception Architecture for Computer Vision," *CoRR*, Vol. abs/1512.00567, 2015. URL <http://arxiv.org/abs/1512.00567>.
- [12] Zeiler, M. D., "ADADELTA: An Adaptive Learning Rate Method," *CoRR*, Vol. abs/1212.5701, 2012. URL <http://arxiv.org/abs/1212.5701>.
- [13] "NWR Data license Germany - Attribution - Version 2.0," <https://www.govdata.de/dl-de/by-2-0>, 2017. Accessed: 2017-09-05.